Nonlinear causal dependencies as a signature of the complexity of the climate dynamics

Stéphane Vannitsem[1,2], X. San Liang[2,3], and Carlos A. Pires[4]

[1]Royal Meteorological Institute of Belgium, Avenue Circulaire, 3, 1180 Brussels
[2]Division of Frontier Research, Southern Marine Science and Engineering Guangdong Laboratory (Zhuhai), China
[3]CMA–FDU Joint Laboratory of Marine Meteorology, Department of Atmospheric and Oceanic Sciences, Fudan University, Shanghai, China
[4]Instituto Dom Luiz, Faculdade de Ciências, Universidade de Lisboa, Lisbon, Portugal

Correspondence: Stéphane Vannitsem (Stephane.Vannitsem@meteo.be)

Abstract. Nonlinear quadratic dynamical dependencies of large-scale climate modes are disentangled through the analysis of the rate of information transfer. Eight dominant climate modes are investigated covering the tropics and extratropics over the North Pacific and Atlantic. A clear signature of nonlinear influences at low-frequencies (time scales larger than a year) are emerging, while high-frequencies are only affected by linear dependencies. These results point to the complex nonlinear collective behavior at global scale of the climate system at low-frequencies, supporting earlier views that regional climate modes are local expressions of a global intricate low-frequency variability dynamics, which is still to be fully uncovered.

1 Introduction

During the last decades, considerable efforts have been devoted to the analysis of the low-frequency variability in the climate system, in order to understand their origin and their implications for long term prediction. This low-frequency variability covers a large range of time scales and processes. A first example at relatively short time scales is the succession of blocked and zonal flows which covers typically time scales from weeks to months (e.g. Hannachi et al., 2017). Another is the low-frequency variability present in the oceans, which impact or interact with the atmosphere, which covers time scales from months to millenia (e.g. Dijkstra and Ghil, 2005). One of the most known ocean-atmosphere interaction is the so called El-Niño-Southern Oscillation (ENSO) dynamics which occurs in the tropical Pacific with typical time scales of a few years, which has considerable impact all over the globe (e.g. Alexander et al., 2002; Newman et al., 2003; Timmermann et al., 2018; Di Lorenzo et al., 2023; Stuecker, 2023). Besides this main mode of ocean-atmosphere co-variability, other low-frequencies are present covering a wide range of time scales, such as the Madden-Julian Oscillation (e.g. Wu et al., 2023); the North Atlantic Oscillation (NAO), Barnston and Livezey (1987) and its quasi-decadal modulation (Da Costa and De Verdiere, 2002); the Quasi-Biennal Oscillation, (e.g. Baldwin et al., 2001); or the Pacific Decadal Oscillation (PDO, Mantua et al. (1997)) and the Atlantic Multidecadal Oscillation (AMO, Enfield et al. (2001)). These low-frequency variabilities are usually characterized through the use of some large scale indices, which summarize the overall dynamics in specific regions of the globe.

In this context, one central question is the link between these different processes: Are there drivers that dominate the overall climate dynamics, like the strong teleconnections of ENSO with the rest of the world, or is there a more intricate set of links and feedbacks that makes the dynamics more complex? Such a question is in general addressed using a process-based causal thinking which is linear by essence: Assume that an observable A is modified, then B is affected which in turn could affect C, and possibly C could affect back A, inducing a feedback loop. Although this way of thinking is very useful in understanding the dynamics of a system, it is not the whole story. One can for instance imagine that the forcing is nonlinear, or that joined (synergetic) effects of several processes could affect a third one, say through a nonlinear product A*B affecting C, which may not be isolated with the approach before. This difficulty has already been realized in climate science, as revealed by different analyses that have been performed in the past decades. A recent example is the analysis of the combined impact of the Southern Annular Mode (SAM) and ENSO on the sea ice in Antarctica Wang et al. (2023). Another example is the dynamics of compound events which need to be activated in order to generate an extreme event (e.g. Zscheischler et al., 2018; Nguyen-Huy et al., 2018). Such types of influences are also revealed by the presence of single and cross-statistical moments of third and fourth-order, for instance between oceanic low-frequency modes (Pires and Hannachi, 2017). These findings suggest that more complicate interactions between climate modes should occur, as for instance discussed in Wang et al. (2009); Tsonis and Swanson (2012); Wyatt et al. (2012); Jajcay et al. (2018) in which synchronization between different climate modes was investigated. The connection between the different indices (or mode of variability) is also emphasized in de Viron et al. (2013) who showed that these modes share a common variability and a strong link with ENSO. Tackling this general problem of links between the different modes of variability necessitates both a clear picture of the (linear and nonlinear) causality involved between these modes, and to clarify the mechanisms that could be at play in such interactions.

In the current work, we will focus on the first aspect by investigating the nonlinear and synergetic dependencies across a set of climate modes. A limited number of key modes is used here in order to have a tractable number of causal links to analyze and at the same time to be comparable to previous works. Eight different indices will be used as in Docquier et al. (2024a), namely the NAO, the Arctic Oscillation index (AO), the Pacific North American index (PNA), the AMO, the PDO, the Tropical North Atlantic index (TNA), the El-Niño 3.4 index, and the QBO index. This is a similar set as in Vannitsem and Liang (2022) without local Belgian temperature, precipitation and insolation indices, and adding the QBO; and also a subset of modes of Silini et al. (2022). The focus is therefore on the Atlantic, Pacific and Tropical basins of the Northern hemisphere.

The causality analysis becomes a popular approach in climate science to evaluate the links between modes of variability. A first very interesting example is the use of the Granger Causality (GC) to evaluate the influence of the Sea Surface Temperature (SST) on the NAO (Mosedale et al., 2006). After this, the GC approach has been used in many occasions, for instance to evaluate the interaction between the ocean and the atmosphere Bach et al. (2019). Another recent example is provided in Zhao et al. (2024) in which two versions of the GC approach are used to understand the interaction between the vegetation and the atmosphere. Several other techniques based on networks or analogs have also been tested with a lot of success, see e.g. van Nes et al. (2015); Kretschmer et al. (2016); Vannitsem and Ghil (2017); Runge (2018); Vannitsem and Ekelmans

(2018); Runge et al. (2019); Di Capua et al. (2020a, b); Huang et al. (2020a, b). Comparisons of different methods of causality analysis are provided in Krakovská et al. (2018) and in Docquier et al. (2024a), and an interesting framework in which several measures based on the dynamics of the information entropy is provided in Smirnov (2022). In the current work, we will use the Liang-Kleeman information flow technique (e.g. Liang, 2014a, 2016), which was used considerably in the recent years in Hagan et al. (2019); Vannitsem et al. (2019); Hagan et al. (2022); Docquier et al. (2022); Vannitsem and Liang (2022); Docquier et al. (2023). There is however a crucial difference is the use of nonlinear observables (or predictors) following the work of Vannitsem et al. (2024) who showed in the context of a reduced-order nonlinear atmospheric system that the method is able to extract the influences originating from nonlinearities. As there are many possible type of nonlinear dependencies, we limit ourselves to use quadratic terms. The justification of this choice lies in the fact that ~~these are the dominant nonlinear polynomials of generic Taylor expansions, and that~~ many climate nonlinearities come from advective quadratic terms.

Section 2 describes the modes of low-frequency variability that will be used in the current study. In Section 3, the tools used to isolate the low-frequency variability in both the atmospheric and oceanic indices and to analyze the dynamical dependencies, are briefly described. The dynamical dependencies (or causality) are discussed in Section 4 with a detailed analysis based first on a reduced set of linear predictors, and second by expanding to a set of predictors containing all quadratic products between indices. Section 5 summarizes the consequences of our findings, and potential research avenues.

2 Data

Eight different regional climate indices characterizing mostly the variability in the Atlantic and Pacific regions of the Northern Hemisphere, are considered. Four of these indices are based on atmospheric variables and four of them are based on oceanic ones. Time series of these indices were retrieved from the Physical Sciences Laboratory (PSL) of the National Oceanic and Atmospheric Administration (NOAA; https://psl.noaa.gov/data/climateindices/list/, last access: July, 10 2024). Monthly values from January 1950 to December 2021 are used in the present work (864 months).

The eight indices are: The Pacific–North American (PNA) index (Wallace and Gutzler, 1981); the North Atlantic Oscillation (NAO) index (Barnston and Livezey, 1987); the Arctic Oscillation (AO), or Northern Annular Mode (NAM), index (Thompson and Wallace, 1998); the Atlantic Multidecadal Oscillation (AMO) index computed based on version 2 of the Kaplan et al. (1998) extended SST gridded dataset using the approach of Enfield et al. (2001); the Pacific Decadal Oscillation (PDO) index (Deser et al., 2010); the Tropical North Atlantic (TNA) index (Enfield et al., 1999); the El Niño3.4 index (for the remainder of the paper, we will mostly refer to this index as “Niño3.4”); and the Quasi-Biennial Oscillation (QBO) index Graystone (1959). These indices are the same as the ones used in Docquier et al. (2024a) in which more details on their characteristics may be found.

3 Methods

3.1 Singular Spectrum Analysis (SSA)

The Singular Spectrum Analysis (SSA) shows similarities with the principal component analysis ~~allowing for constructing key spatial modes known as Empirical~~ where a covariance matrix is diagonalized. In the SSA, the lag-covariance matrix of a single time series is diagonalized where the eigenvectors or Temporal-Empirical Orthogonal Functions (~~EOFs) . The purpose of SSA is however to isolate the temporal dominant modes~~T-EOFs) are finite time sequences providing the more frequent and higher amplitude finite time-spells of that variable. To construct them, the time series, $X(i)$ with $i = 1, ..., N$, of each index, is embedded into a phase space of dimension, say M, using a delay-coordinate state vector $Y(t) = [X(t-M+1), ..., X(t)]$, whose coordinates are the successive values in the time series (e.g. Broomhead and King, 1986; Vautard et al., 1992; Fraedrich et al., 1993; Ghil et al., 2002). The evolution in phase space is then obtained by sliding the M-window in time. This operation can be expressed as an eigenvalue problem of the following $M \times M$ Toeplitz matrix:

$$\begin{pmatrix} T(0) & T(1) & T(2) & ... & T(M-1) \\ T(1) & T(0) & T(1) & ... & T(M-2) \\ .... & & & & \\ T(M-2) & T(M-3) & T(M-4) & ... & T(1) \\ T(M-1) & T(M-2) & T(M-3) & ... & T(0) \end{pmatrix} \tag{1}$$

where each matrix entry (i,j) is the lag-covariance $cov(X(t), X(t+|i-j|))$. The eigenvalues and eigenvectors can then be computed. These eigenvectors characterize the dominant modes within the M-window, like intermittent oscillating spells with periods less than M. The window M is in general fixed to $1/10$ of the length of the time series in order to have enough statistics for estimating the covariance matrix. In the current work, it is fixed to 240 months, a bit longer than the default value in order to resolve decadal time scales. More information on the method is provided in Vautard et al. (1992) and Ghil et al. (2002).

For each index, we compute the SSA spectrum and evaluate visually each of the 40 SSA modes corresponding to the 40 dominant eigenvalues. These different modes have a time length of 240 months (the M-window mentioned earlier). If the dominant period in each mode evolution is shorter than a year, the mode is discarded, the idea being to keep the low-frequency variability large than a year, only. After filtering out the modes displaying high frequencies~~with dominant visible periods smaller than a year~~, we end up with new low-frequency variability series of the original monthly anomalies of the climate indices (the monthly mean has been removed before the application of the SSA). The modes that are kept in the low-frequency signal are listed in Table 1~~, after exploring the 40 first modes (i. e the temporal principal components (T-PCs) of the vector $Y(t)$) for each series.~~ . There is here a certain degree of arbitrariness as we discard sometimes modes that display a mix of low-frequency and high-frequency variabilities. We do believe however that the essence of the LFV dynamics is well captured by our selection. Note also that the LFV of most of the oceanic modes are essentially concentrated in the dominant SSA modes of variability.

In order to evaluate the impact of choosing specific SSA modes rather than others on the causality analysis, we have also considered arbitrary choices of modes, namely the even modes $2k$ and the odd modes $2(k-1)+1$, for $k=1,\ldots,20$. The analysis reveals that considerably less significant influences from nonlinearities are detected (5 instances for the odd modes and 2 instances for the even modes), indicating that these arbitrary choices are not providing optimal results. With such choices, high and low frequencies are again mixed up, leading to a rather suboptimal result. The presence of high frequencies is indeed hindering the proper detection of dependencies given the short time series.

Table 1. Set of SSA modes kept in the reconstruction of the low-frequency variability of the monthly anomalies of the climate indices displayed in Fig. 1

Indices	LFV modes
NAO	3, 11,12, 13, 14, 17, 18, 29, 30
AO	1, 2, 3, 4, 7, 12, 13, 18, 19
PNA	3, 4, 14, 17, 18, 21, 24, 25, 29, 31, 32, 35, 36, 39
AMO	1, 2, 3, 4, 5, 6, 10, 11, 12, 13, 14, 15, 16, 17, 18, 19, 20
PDO	1, 2, 3, 4, 5, 6, 7, 8, 9, 10, 11, 12, 15, 16, 17, 18, 19, 20
TNA	1, 2, 3, 4, 5, 6, 7, 8, 9, 10, 11, 12, 13, 14, 15, 16, 20
Niño3.4	1, 2, 3, 4, 5, 6, 7, 8, 9, 10, 11, 12, 13, 14, 15, 16, 17, 18, 19, 20
QBO	1, 2, 3, 4, 5, 6, 7, 8, 9, 10, 11, 12, 13, 14, 15, 16, 17, 18, 19, 20

Note that a sensitivity test has also been performed by removing the trends in temperature for Niño3.4 index, with little impact on the results discussed below.

3.2 Rate of information transfer

Liang has developed a theory on causal dependencies in the context of nonlinear stochastic systems based on the estimation of changes of the information entropy of the system, leading to an expression for the rate of information transfer between variables (Liang and Kleeman, 2005; Liang, 2014a, b, 2016, 2021). A simpler expression was subsequently deduced for linear stochastic systems forced by additive noise, allowing for direct estimation on observational data as discussed in Liang (2014b, a, 2021). The latter approach is also known as the Liang's method. It has been applied in various climate contexts (Vannitsem et al., 2019; Vannitsem and Liang, 2022; Docquier et al., 2022, 2023, 2024a). A recent extension of the theory allowing for estimating the rate of information transfer based on conditional expectations has been performed in Pires et al. (2024) and tested in the context of a reduced order model displaying deterministic chaos in Vannitsem et al. (2024). In the latter, an extension of the Liang's method for time series analysis is also tested allowing for incorporating nonlinear predictors.

Let us consider S time series, X_i, $i=1,...,S$, having N data points, $X_i(n)$, $n=1,2,...,N$, recorded at regular time step Δt. A forward temporal derivative can be computed as

$$\dot{X}_i(n) = \frac{X_i(n+1)-X_i(n)}{\Delta t} \tag{2}$$

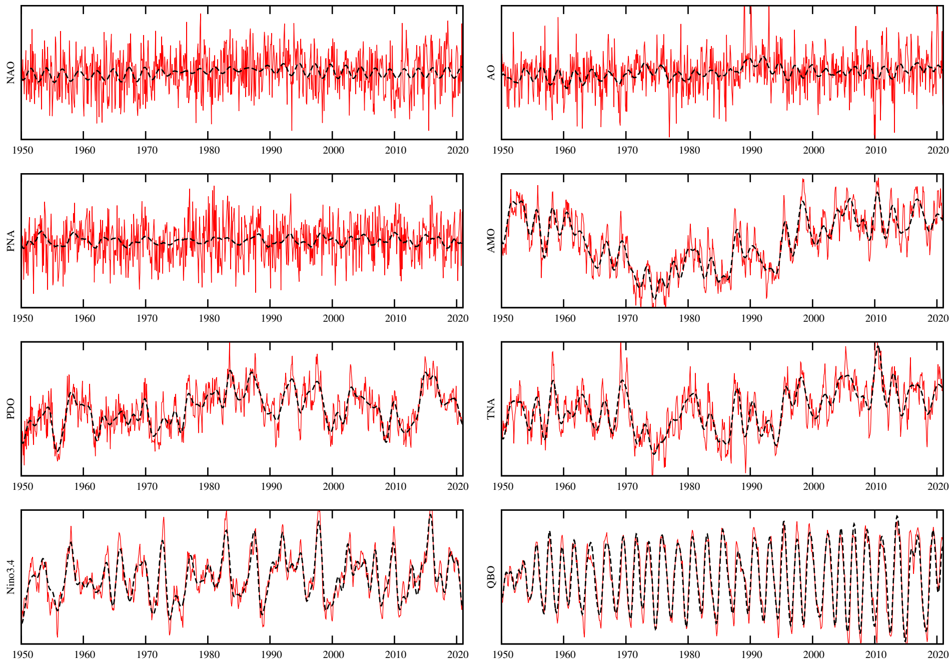

Figure 1. Original (red) and filtered (black) monthly anomaly time series of the climate indices, covering the period 1950-2021.

Let us denote C_{ij} as the sample covariance between X_i and X_j, and $C_{i,dj}$ the sample covariance between X_i and the temporal derivative $\dot{X}_j$. It has been shown that the estimator of the rate of information transfer from variable X_j to variable X_i, is

$$\hat{T}_{j\to i} = \frac{1}{\det \mathbf{C}} \cdot \sum_{k=1}^{S} \Delta_{jk} C_{k,di} \cdot \frac{C_{ij}}{C_{ii}}, \tag{3}$$

where Δ_{jk} are the co-factors of the covariance matrix $\mathbf{C} = (C_{ij})$, and $\det \mathbf{C}$ is the determinant of $\mathbf{C}$. Note that this is valid under the approximation that (X_i, X_j) is jointly Gaussian, otherwise the term C_{ij}/C_{ii} must be replaced by $E[d/dX_i(E(X_j|X_i))]$, relying on nonlinear conditional expectations as in Pires et al. (2024).

Generically causation ~~implies~~ is assumed to imply correlation, but correlation clearly does not imply causation. This feature nicely emerges in the mathematical expression (3), when considering two time series only as discussed in Liang (2014a). So the significance test allowing for evaluating causal dependencies consists in computing the rate of information transfer and check whether it is significantly different from zero. Several approaches may be used, and here a bootstrap method with replacement is used (Efron and Tibshirani, 1993), in a similar way as in Vannitsem et al. (2019). The level of confidence is fixed here to 1% in order to avoid as far as possible false positive, but as indicated in Docquier et al. (2024a), false negative may arise when the number of predictors is high and the time series short. This caution is most probably applicable here, and therefore some nonlinearities may not be properly isolated (some false negative).

A normalization of the rate of information transfer is also performed in such a way that the influences of the different variables on the target can be evaluated on the same ground. It will provide a percentage of influence. The normalization factor in the multivariate case is as in Liang (2021):

$$Z_i = \sum_{k=1}^{S} |\hat{T}_{k\to i}| + \left|\frac{dH_i^{noise}}{dt}\right| \tag{4}$$

where $\left|\frac{dH_i^{noise}}{dt}\right|$ is the contribution of the noise of the underlying linear stochastic model.

The relative transfer of information from X_j to X_i is given by,

$$\tau_{j\to i} = \frac{\hat{T}_{j\to i}}{Z_i} \tag{5}$$

Note that the time series used are relatively short. This implies that some links could not be detected as the uncertainty around the value of the rate of information transfer may be large. Given that caveat, some dependencies of the method on the bootstrap sample have been explored in Docquier et al. (2024a). They concluded that 1000 bootstrap samples are a good choice to detect causal links on short climate time series.

Another potential difficulty is the number of predictors. In Docquier et al. (2024a), it was indicated that to get a good detection, a small number of predictors should be used (of the order of maximum 10). It was however shown in the more theoretical study of Vannitsem et al. (2024) that using a combination of linear and nonlinear terms up to 44 predictors, still allow us to get meaningful results. The different conclusions reached are probably associated with the different setups used in both studies, and this question should be further addressed in the future.

The approach proposed by Liang allows for constructing a network of directional connections between observables that are measured concomitantly. This approach is distinct to techniques that assume that causation should be based on a time lag between events like the classical network approach (Runge et al., 2019; Di Capua et al., 2020a). ~~The Liang's approach seems therefore distinct to the usual view that in a causal relationship the causing event should arise before the caused event with a lag much larger than the time step. In fact both views can be reconciled if one realizes that the Liang's approach is isolating links between events for time lags going to zero. In that sense the method is also causal, with the strong advantage that there is no specific dependence on a lag.~~ If real processes indeed display a lag – like for instance in the propagation of a wave –, the information will propagate from one point to another, and this will be isolated in the Liang's method through a specific path through the network. As in reality we usually do ~~no~~ not have all variables (at all grid points for instance), this could not show up, but filtration through (spatial or temporal) averaging ~~of~~ or frequencies selections should help in disentangling the impact of one distant observable to another, as for instance in Vannitsem and Liang (2022).

Note also that the sign of influence also contains interesting information: when positive, it means that the predictor is inducing an increase of uncertainty (or variability) of the target; while when it is negative, the predictor reduces the uncertainty (variability) of the target. This information is however quite sensitive to the set of predictors used as discussed in Vannitsem et al. (2024). We will therefore not discuss that in details, except if outstanding features are emerging.

4 Results

4.1 Influence on an atmospheric index: NAO

Let us first consider the influence on one specific climate index, the NAO. Figure 2 displays the application of the Liang's method (Eq. 5) to the original NAO time series, as well as to the low-frequency filtered data. A first remark is that the only influence detected at the 1% level on the original series is originating from the AO, while correlation is statistically significant for AO, AMO and TNA. This result is in agreement with Docquier et al. (2024a). Note that we used 1% in order to reduce false positive cases, in particular when the number of predictors used is large. When the analysis is applied to the low-frequency variability of the series, the influence of AO does not appear anymore, while the influence of PNA and QBO emerge, together with correlations with all the other indices. The fact that the AO influence disappears probably reflects that it mostly acts on shorter time scales (not present in the LFV series anymore), while PNA and QBO on the low-frequency NAO signal. The influence of TNA is consistent with the barotropic teleconnection mechanism proposed in Okumura et al. (2001).

This linear approach of course could miss the impact of the joint influence or co-variability of indices. In Vannitsem et al. (2024) this question was addressed in the context of reduced-order atmospheric model, and it was shown that joint influences in the form of polynomial nonlinearities could be very large and dominate the sources of information transfer. To deal with that aspect in the context of time series analysis, they also propose to use new types of observables in the context of the Liang's approach as products of system's variables. It was indeed found that if nonlinearities are not playing a role in the dynamical equations, the corresponding rate of information transfer obtained on the time series generated by the model would be negligible. This result provides some hope to be able to isolate nonlinear influences in the real atmosphere too.

To disentangle the role of nonlinearities in the context of ~~our~~ the 8 climate indices, all combinations of quadratic terms are constructed. This choice is made ~~as~~ since in many dynamical systems ~~where~~ such nonlinearities are ~~usually~~ present. These ~~are also the second order terms of Taylor expansions in many more sophisticated nonlinearities like exponentials and logarithmic functions often used to describe explosive or saturating contributions. Note that in what follows and in the figures, the product between indices is denoted with a '*' and the square of an index as '**2'~~quadratic nonlinearities are typically associated with the presence of nonlinear advection terms in the classical conservation laws (momentum equation, thermodynamic equation, ...), as for instance illustrated in the work done recently in the context of the Charney – Straus model Vannitsem et al. (2024) . These however could be viewed as restrictive and tests should be done in the future to evaluate the impact of higher order or more complicate nonlinearities.

Figure 3a displays the application of the Liang's approach with the additional 36 quadratic observables on the original series. The only influence emerging in this panel is associated with the AO index as for the analysis based on the purely linear approach of 2. It is stricking to see that there is no quadratic nonlinearity which emerges here as these are very close to 0. This negative result is very useful as it shows that if there is no nonlinear influence in the form considered here, it will not show up, and that the linear dependence on AO is a robust feature of the influence to NAO in the original series.

An even more ~~stricking~~ striking result is found when only investigating the low-frequency variability of these indices. Figure 3b displays the results with the nonlinear observables. As for the previous discussion of Figure 3a, the dependencies of

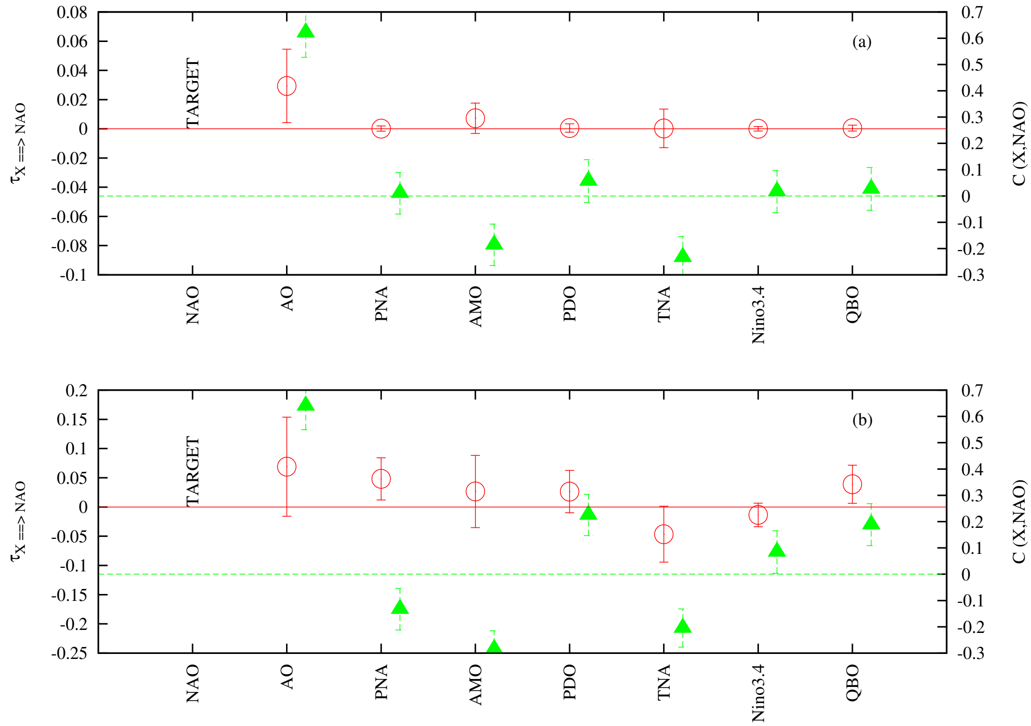

Figure 2. The rate of information transfer (left y-axis, red open circles) and the correlation (right y-axis, green full triangles) are plotted as a function of the observables for the targeted observable (labelled TARGET in the plot): the NAO. Panels (a) and (b) are for the original and LFV time series, respectively.

NAO from PNA and QBO are again emerging, but additional dependencies are found from PDO and 7 different nonlinearities: ~~PNA*TNA, TNA*QBO, PNA*AMO, AMO*QBO, AMO**2, PNA*QBO, AO*QBO~~PNA TNA, TNA QBO, PNA AMO, AMO QBO, AMO^2, PNA QBO, AO QBO. In all those cases correlation is significantly different from zero, though the reverse is not true as expected (i.e. correlation does not imply causation). The PDO influence on the low-frequency variability of NAO is consistent with the findings of Nigam et al. (2020). The influence of QBO is also consistent with the important role played by the stratosphere as found in Ambaum and Hoskins (2002); Scaife et al. (2005). This indicates that the influence of the Atlantic ocean through TNA and AMO are only emerging jointly with PNA and QBO, and through the quadratic amplitude of AMO. At the same time the influence of AO is now mediated through the joint influence with QBO. Interestingly, the nonlinear joint influence of the QBO with the Atlantic multidecadal variability is consistent with the results presented in Omrani et al. (2014, 2022) who demonstrated the essential influence of the stratosphere on the extra-tropical atmospheric response to ocean variability. The latter interesting investigation of joint influences, consistent with our findings, should be extended to the other nonlinearities uncovered in the current analysis. A visual picture of the dependencies is provided in Fig. 4.

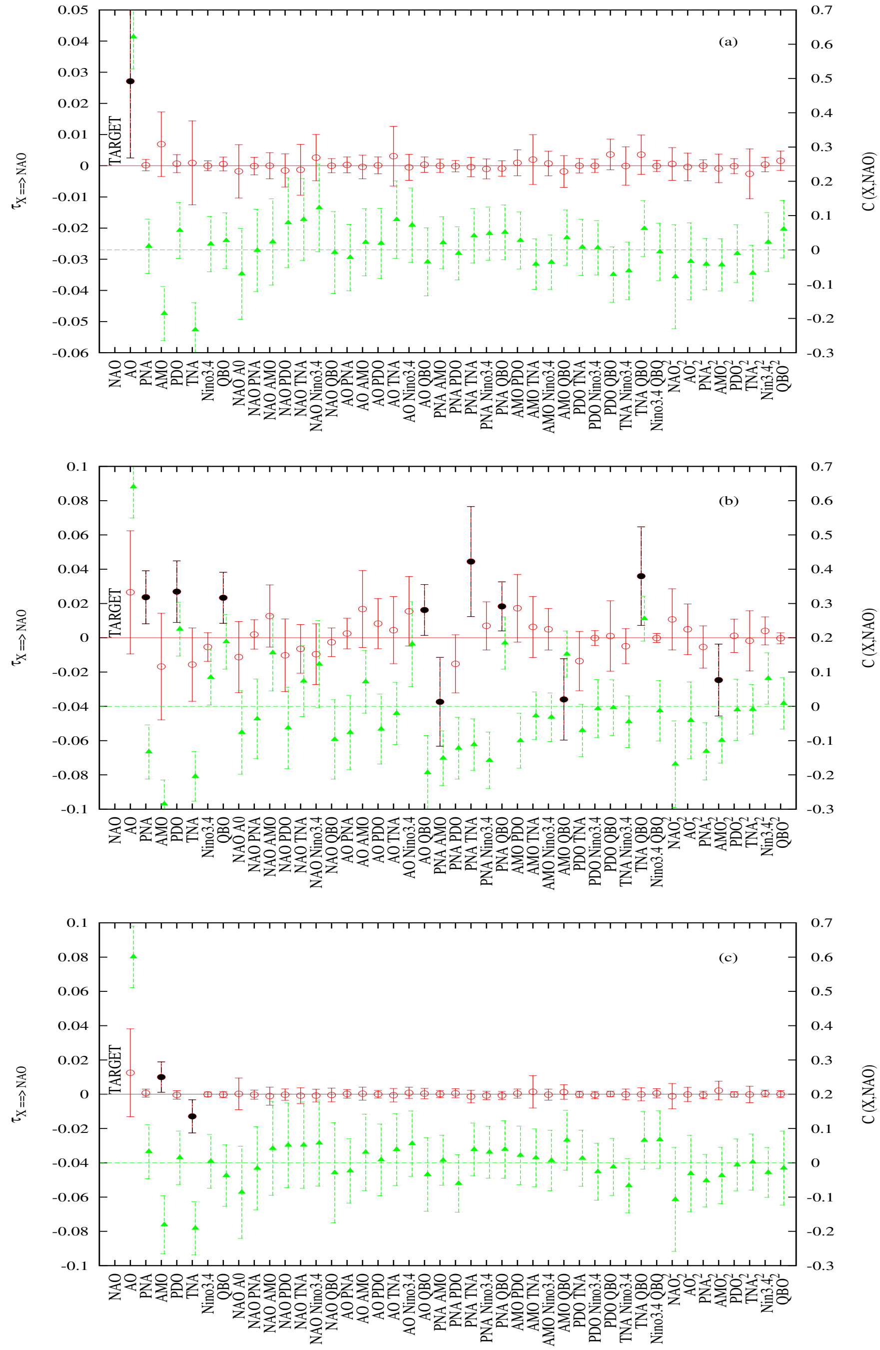

Figure 3. The rate of information transfer (left y-axis, red open circles) and the correlation (right y-axis, green full triangles) are plotted as a function of the observables for the targeted observable (labelled TARGET in the plot): the NAO. Panels (a), (b) and (c) are for the original, the LFV and the high-frequency time series, respectively. The observable set is composed of 7 linear terms and 36 nonlinear quadratic terms, all listed along the x-axis. The points in black refer to the significant dependencies at the 1% level.

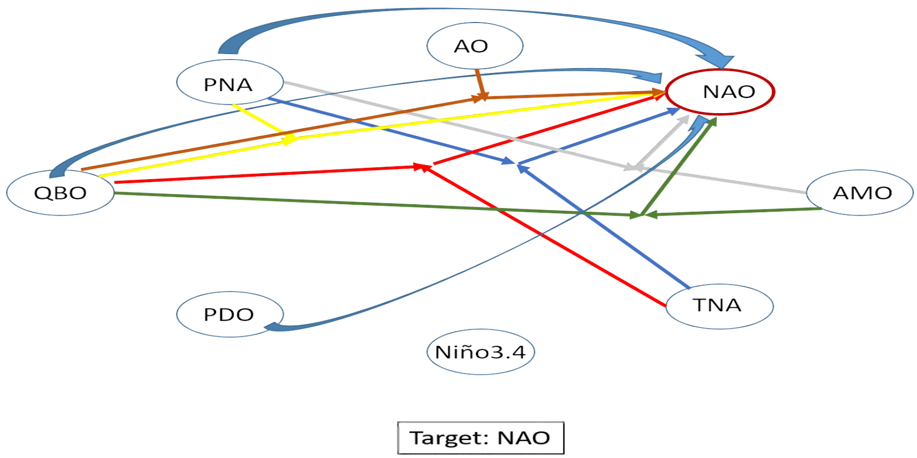

Figure 4. A visual representation of the linear and nonlinear influences from the set of indices to the NAO for the low-frequency variability dataset. the curved plain arrows refer to the linear influence, the triple straight arrows with the same colors refer to the influence of the quadratic nonlinearities: two straight arrows are emanating from two indices, joining somewhere in between the indices, and from there the third straight arrow indicates the target.

Related to the sign of influence, it is interesting to note that all nonlinear predictors involving the AMO show a negative influence on the NAO. This feature suggests that the AMO, in combination with several indices, tends to reduce the variability of the NAO. This conjecture should be checked in the future either through additional analyses with a wider set of indices, and through a process-based analysis as done for instance in Omrani et al. (2014, 2022).

A test on the high-frequency variability computed as the difference between the original series and the LFV series is also performed to clarify whether nonlinearities are also playing an important role at these frequencies. Two weak linear dependencies emerge from the AMO and the TNA, suggesting some quick response of the NAO to the Atlantic ocean temperature, but no nonlinear influences emerge here. This interesting feature suggests that nonlinear couplings between the different climate modes are only present at long time scales. This point is also taken up in the next section.

Here a few important considerations are in order:

- As in Vannitsem et al. (2024), the use of new nonlinear observables could also modify the contributions of linear influences as for instance the emergence in Fig. 3b of the influence of PDO and the reduction of TNA influence in the low-frequency NAO signal. The modifications can be either present in the average influence or in the amplitude of the confidence intervals

- A few influences in the low-frequency variability of climate indices could emerge only through nonlinearites, revealing the joint impact of pairs of indices

- The high-frequency variability of the NAO is only influenced through linear terms associated with the ocean variability over the Atlantic

– The fact that the use of the nonlinear terms on the original and high-frequency series does not provide any substantial influence suggests that the scheme proposed is unlikely to produce spurious influence through nonlinear terms if indeed not present

4.2 Influence on an oceanic index: El Niño

Let us now perform the same analysis for the well-known dynamics in the tropical pacific. Figure 5a shows the influence at the 1% level of confidence of PNA and TNA, again this is in agreement with Docquier et al. (2024a). If one considers the low-frequency variability only, the influence of PNA is not statistically significant at the 1% level but well at the 5% level. On the other hand there is a very strong influence of TNA and PDO with amplitudes of -0.181 and -0.163, both accounting for more than 35% of the total influence. Both characterize ocean processes known to be connected with the dynamics of El-Niño Levine et al. (2017); Park and Li (2019); Johnson et al. (2020).

Figure 6a displays the analysis done with all the quadratic nonlinearities. First there is no specific nonlinearity which emerges here. Second the dominant influences is now in TNA at 1% level, while PNA will only appear at a lower level of confidence. As for NAO, the extension of the analysis of the original series using the nonlinear terms did not show any nonlinear influence, and only reveals the influences already isolated with the original variables.

Let us now turn to the nonlinear analysis of the low-frequency series (Figure 6b). The influences of PDO and TNA still remains dominant, although with lower amplitudes. Interestingly, most of the nonlinearities that show significant influence (~~AO*PDO, AO*Niño3~~AO PDO, AO Niño3.4, ~~AO*PNA, AO**2~~AO PNA, AO^2) are involving the influence of the AO, the only additional nonlinearity is Niño3.4~~**2~~^{2}. This influence clearly does not emerge in the purely linear analysis, suggesting that the AO influence the low-frequency variability of El Niño only in conjunction with other key climate indices. To our knowledge, this specific influence of AO on El Niño was not reported before, which is worth exploring further in the future. The additional positive causation comes from the nonlinear term Niño3.4~~**2~~^{2}, which is related to the positive El-Niño skewness Burgers and Stephenson (1999) and the tendency for extreme El-Niños or La-Niñas to generate future El-Niños, 2-3 years later, as shown by cross-bicovariance and bi-spectral analysis of El-Niño time series Pires and Hannachi (2021). A visual picture of the dependencies on Niño3.4 is provided in Fig. 7.

Interestingly, there is no influence of any linear or nonlinear predictor at high-frequencies as illustrated in Figure 6c. This result first demonstrates that only low-frequency variability in the other indices are influencing the dynamics of El-Niño 3.4, and second, on more technical grounds, that false positive can indeed be rare, giving confidence in the analyses done on the low-frequency variability indices. Similar remarks as the ones listed at the end of the previous section are also in order here.

4.3 Influences on the other climate modes

Concerning the other indices, a similar analysis has been performed, and a summary of the findings is given in Tables 2 and 3 for the analysis based on the 8 original of filtered series only, and based on the extended set of observables containing the 8 variables themselves and the nonlinearities already described in the previous sections. Note that all detailed figures are given in the Supplementary material.

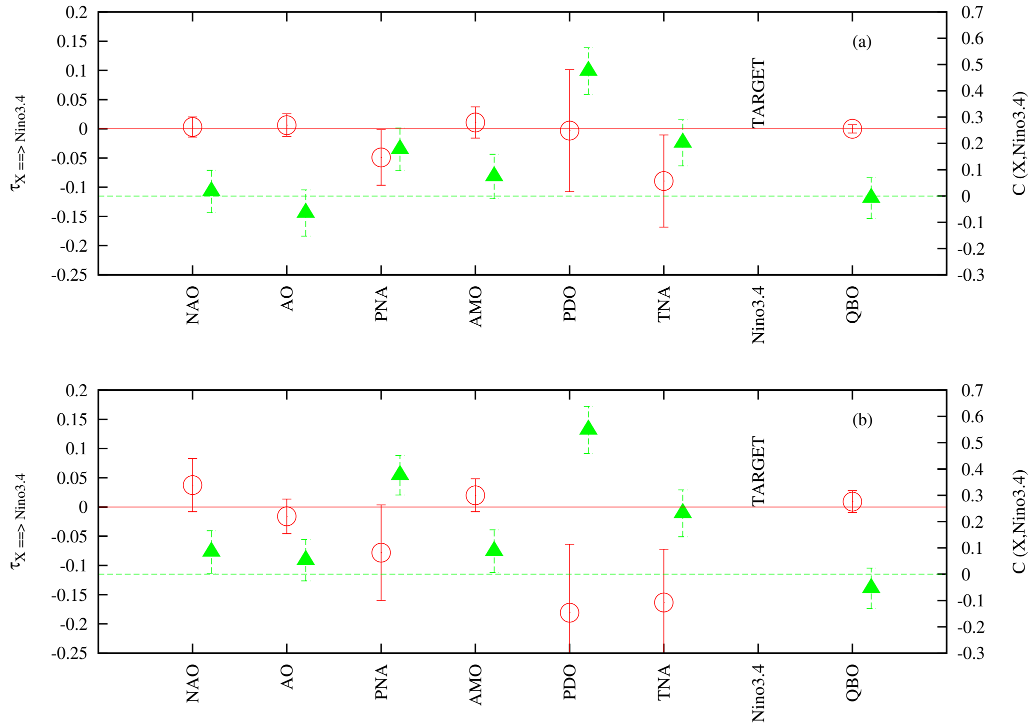

Figure 5. The rate of information transfer (left y-axis, red open circles) and the correlation (right y-axis, green full triangles) are plotted as a function of the observables for the targeted observable (labelled TARGET in the plot): the Niño3.4. Panels (a) and (b) are for the original and LFV time series, respectively.

For AO, there is no influence detected on the original series. Turning now on the filtered ones containing the low-frequency variability of all series, the linear analysis reveals the presence of influence of NAO and TNA. If one uses all nonlinearities, the influence of NAO still remains a a linear term but not TNA. TNA now appears in conjunction with the influence of QBO. Niño3.4 also emerges through the nonlinearities in conjunction with NAO and PNA. Finally QBO and PNA are also emerging as influencing linearly AO.

PNA is influenced by Niño3.4 (as also indicated in Silini et al. (2022)) and AO whatever the original or filtered series are analyzed and whatever the set of predictors used (linear or nonlinear). This shows the robustness of these influences for both the full variability series and its low-frequency counterpart. When the nonlinear analysis is performed on the filtered series, a large set of new influences emerge: PDO is the dominant influence which was not present in the linear analysis; the NAO is also emerging with a linear influence; and a bunch of nonlinear influences involving the NAO, AMO, TNA, PDO and QBO. Here all indices show influences either through linear or nonlinear terms.This reflects the complexity of the dynamics of PNA.

The AMO shows an overal strong influence from TNA whatever the series and predictor sets used. When the nonlinear analysis of the filtered series is performed, a set of linear and/or nonlinear influcences emerge from PNA and NAO, together

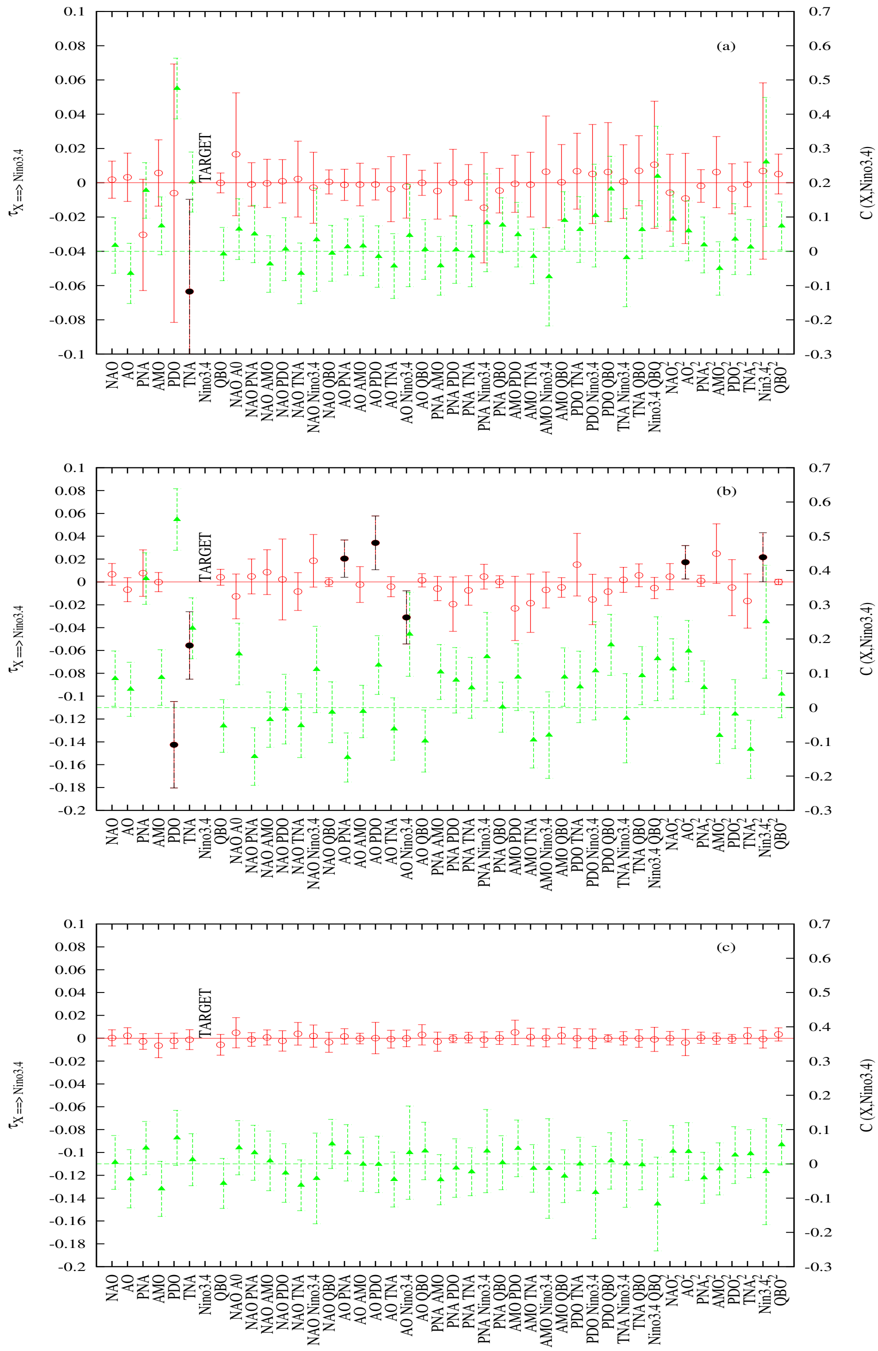

Figure 6. The rate of information transfer (left y-axis, red open circles) and the correlation (right y-axis green full triangles) are plotted as a function of the observables for the targeted observable (labelled TARGET in the plot): the Niño3.4. Panels (a), (b) and (c) are for the original, the LFV and the high-frequency time series, respectively. The observable set is composed of 7 linear terms and 36 nonlinear quadratic terms, all listed along the x-axis. The points in black refer to the significant dependencies at the 1% level.

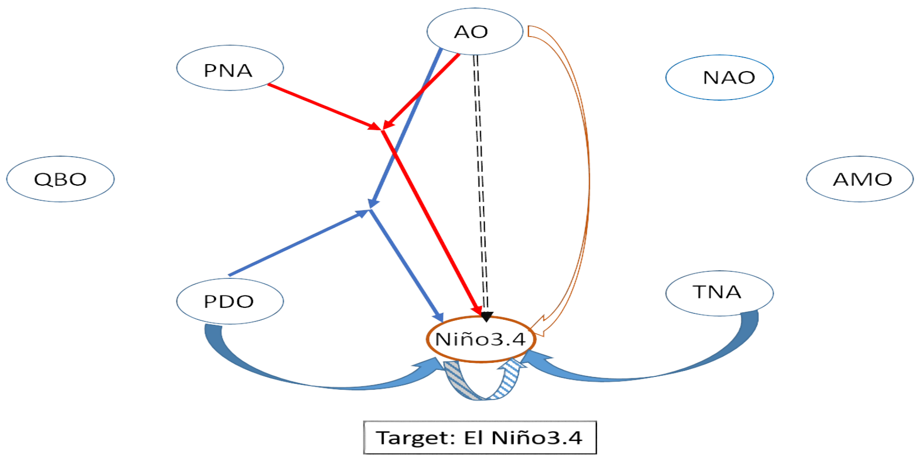

Figure 7. A visual representation of the linear and nonlinear influences from the set of indices to the El Niño3.4 for the low-frequency variability dataset. the curved plain arrows refer to the linear influence, the triple straight arrows with the same colors refer to the influence of the quadratic nonlinearities: two straight arrows are emanating from two indices, joining somewhere in between the indices, and from there the third straight arrow indicates the target. The double dashed straight (black) arrow indicates the influence of the product between the source and the target. The empty curved arrow indicates the quadratic influence of the source, while the striped curved arrow the quadratic influence of the target.

Table 2. List of climate indices that have a significant influence on the targets mentioned in the first row. These are listed by order of importance based on the mean value of the rate of information transfer (over 1000 bootstraps). These estimates are shown in Figs 2 and 5, as well as in the figures in the supplementary document. The value for the dominant information transfer is given between parentheses.

Targets:	**NAO**	**AO**	**PNA**	**AMO**	**PDO**	**TNA**	**Niño**	**QBO**
Influences from linear predictors	AO(.029)	-	AO(.013) Niño	TNA(-.28)	Niño(.090) AO	AMO(.15) Niño AO	TNA(-.089) PNA	-
Influences from linear predictors (LFV Series)	PNA(.048) QBO	NAO(-.28) TNA	Niño(.22) PDO NAO AO	TNA(-.34)	Niño(.22) NAO TNA AO QBO	Niño(.15) AMO PNA AO	PDO(-.18) TNA (PNA)	NAO(-.09) (TNA)

with a quadratic self-influence. Interestingly a strong NAO is likely to influence AMO through the term NAO**2 revealing the importance of extreme NAO events on the AMO, while the influence of PNA emerges only in conjunction with an amplification of AMO.

For PDO, the influences of Niño3.4 and AO are always detected in the different analyses performed. The analysis confirms results already reported in Silini et al. (2022) and Vannitsem and Liang (2022). When the filtered data are used, additional linear influences are detected from TNA, NAO and QBO, together with some nonlinear dependencies combining AO, NAO, AMO and PDO.

For TNA, a similar picture is found with influences from Niño3.4, AMO and AO found in all analyses performed, either linear or nonlinear, or using the original or filtered data. The influence of PNA is emerging only in the analysis of the filtered dataset, and additional influences from QBO and PNA are felt through nonlinearities. Note also that the AMO does not appear as a linear influence in the fully nonlinear analysis of the filtered data, but rather as the square of this index. The later reveals that strong influence of AMO is only felt when the AMO has high amplitude.

Finally for QBO, no influences are felt using the original dataset, while it appears on the filtered data, with a dominant influence of NAO with the linear analysis. For the fully nonlinear analysis, a large variety of nonlinearities are influencing QBO in which all climate modes are involved. Note however that these influences are always very small, even if significant.

The analysis based on the high-frequency time series reveals that there is no nonlinear influences affecting the different indices: For NAO, weak infuences on AMO and TNA are detected; For AO, a weak influence of TNA; For PNA, weak inlfuences of AO and PDO; for the AMO, a large influence of TNA; for PDO, weak inluence of AO; for TNA, influences by AO and AMO; and finally for QBO, no influence detected.

All these complicate nonlinear dependencies between the climate modes are also worth exploring more on a process dynamics perspective as it was done for the interaction between the stratosphere, the troposphere and the ocean as in Omrani et al. (2014).

5 Conclusions

This work ~~extends the analyses done in Vannitsem and Liang (2022); Docquier et al. (2024a) in~~ investigates the quadratic nonlinear influences on a set of climate indices~~by allowing to isolate nonlinear influences of quadratic predictors built as products of the~~. This is done by considering, as predictors in the analysis, products of indices. This extension to nonlinear predictors has proven to be successful in the idealized context of a ~~reduced-order atmospheric model (Vannitsem et al., 2024). A few~~ reduced order model Vannitsem et al. (2024). The analysis reveals that nonlinearities are indeed coupling the low-frequency variability of climate indices, revealing the complexity of the climate system at time scales from years to decades. A few additional key conclusions may be drawn from this analysis:

- The method of Liang, extended to nonlinear observables, is indeed an interesting approach to disentangle the impact of nonlinearities on the evolution of the climate modes, as suggested in Vannitsem et al. (2024)

- The analysis of the climate modes indicates that the low-frequency variability of the climate system over the Northern tropics-extratropics dynamics is also involving nonlinearities that are reflecting the joint influences of several climate modes on the target one. This may explain the "nonstationarity" of influences often raised in the climate system, e.g.

García-Serrano et al. (2017), related to conditional influences of one climate mode given the evolution of a second mode. For instance the influence of AO on Niño3.4 can only be seen depending on the actual state of PDO, Niño3.4 and PNA (see table 3). The latter result is worth exploring further through process-based analyses

- Robust linear influences have also been isolated for both the original and filtered (LFV) time series, and whatever the number of predictors used (linear and nonlinear)

- Intricate nonlinear relations between all the modes are emerging at low-frequencies, suggesting that these modes and their dynamics cannot be looked as isolated or as pure forcing and forced subsystems

The last conclusion points to the general question of the nature of the dynamics of the climate system on time scales from years to decades, or in other words, what processes are driving others. In view of the linear and nonlinear dependencies disentangled in the current work at low-frequencies, the number of connections and the complexity of the interplay of processes that could join "force" to influence a third one through nonlinearities, are high. This is reminiscent of triadic wave resonances in fluid dynamics Pires and Perdigão (2015). This suggests in turn that the simplistic viewpoint of having forcing and forced subsystems should be revisited, and the climate system at low-frequencies should be rather viewed as a nonlinear dynamical system with a collective behavior all over the globe. This vision of the large-scale climate system supports similar visions found in earlier works on the collective behavior of the different large scale atmospheric and ocean processes, e.g. (Wang et al., 2009; Tsonis and Swanson, 2012; Wyatt et al., 2012; de Viron et al., 2013; Runge et al., 2019; Silini et al., 2022).

In the current analysis, a limited set of modes have been considered. This of course has implications as some important connections would have been missed, for instance with the Indian Ocean, with the large scale dynamics in the Southern Hemisphere or with the Northern circumglobal pattern (e.g. Ding and Wang, 2005; Ding et al., 2017; Di Capua et al., 2020a). Other multiple synergies among oceanic basins can emerge like that between the Pacific and Atlantic El-Niños and the AMO as shown by Martín-Rey et al. (2014). The absence of these large-scale modes may also affect the linear and nonlinear dependencies isolated in the current work. Extending to a larger number of large-scale modes as in de Viron et al. (2013) and Silini et al. (2022) is certainly worth doing in the future, but more importantly is to figure out the set of modes would be enough to have a sufficiently accurate and complete description of the global climate dynamics. This is left as an key open research topic. ~~This would also allow~~ This knowledge could also provide hints on the nonlinearities that would be useful to build a ~~reduced-order data-driven climate model that could potentially help in understanding the global climate evolution~~data driven model of the large scale climate indices. A possible avenue is to use techniques of machine learning, with the help of information theory to isolate these dominant modes and their interactions, e.g. (Liang et al., 2023; Tyrovolas et al., 2023). Another path is to build simplified stochastic models as for instance in a recent application Kravtsov et al. (2005). Finally, the modifications of these influences with climate change should be investigated, as for instance in Stips et al. (2016); Docquier et al. (2022, 2024b).

Finally, it would be very useful to compare these results using another approach as the network approach developed and used in Runge (2018); Runge et al. (2019); Di Capua et al. (2020a); Docquier et al. (2024a), and check whether similar nonlinearities (with lags) at low-frequencies would emerge.

Code and data availability. The original climate indices are available at https://psl.noaa.gov/data/climateindices/list/. The SSA code is available on the website https://research.atmos.ucla.edu/tcd/ssa/, while the Fortran version of the code for computing the transfer of information and the filtered data are available upon reasonable request to the main author.

Author contributions. SV, XSL and CAP designed the study. SV retrieved the climate indices and created the filtered low-frequency dataset. SV made the computations with the datasets. SV led the writing of the manuscript, with contributions from all co-authors. SV created all figures. All authors participated to the data analysis and interpretation.

Competing interests. The authors have no competing interest.

Acknowledgements. Stéphane Vannitsem and Carlos A Pires are partly supported by ROADMAP (Role of ocean dynamics and Ocean-Atmosphere interactions in Driving cliMAte variations and future Projections of impact-relevant extreme events), a coordinated JPI-Climate/JPI-Oceans project. Stéphane Vannitsem acknowledges the funding support from BELSPO under contract B2/20E/P1/ROADMAP. Carlos Pires is supported by Portuguese funds: Fundação para a Ciência e a Tecnologia (FCT) I.P./MCTES through national funds (PIDDAC) – UIDB/50019/2020 (https://doi.org/10.54499/UIDB/50019/2020), and LA/P/0068/2020 (https://doi.org/10.54499/LA/P/0068/2020), and the project JPIOCEANS/0001/2019 (ROADMAP). X. San Liang is partially supported by National Science Foundation of China (NSFC) (Grant #42230105) and Southern Marine Science and Engineering Guangdong Laboratory (Zhuhai) (#313022005 and #SML2023SP203).

References

Alexander, M. A., Bladé, I., Newman, M., Lanzante, J. R., Lau, N.-C., and Scott, J. D.: The atmospheric bridge: The influence of ENSO teleconnections on air–sea interaction over the global oceans, J. Climate, 15, 2205–2231, https://doi.org/10.1175/1520-0442(2002)015<2205:TABTIO>2.0.CO;2, 2002.

Ambaum, M. H. P. and Hoskins, B. J.: The NAO Troposphere–Stratosphere Connection, Journal of Climate, 15, 1969 – 1978, https://doi.org/10.1175/1520-0442(2002)015<1969:TNTSC>2.0.CO;2, 2002.

Bach, E., Motesharrei, S., Kalnay, E., and Ruiz-Barradas, A.: Local atmosphere-ocean predictability: Dynamical origins, lead times, and seasonality, Journal of Climate, 32, 7507–7519, https://doi.org/10.1175/JCLI-D-18-0817.1, 2019.

Baldwin, M. P., Gray, L. J., Dunkerton, T. J., Hamilton, K., Haynes, P. H., Randel, W. J., Holton, J. R., Alexander, M. J., Hirota, I., Horinouchi, T., Jones, D. B. A., Kinnersley, J. S., Marquardt, C., Sato, K., and Takahashi, M.: The quasi-biennial oscillation, Reviews of Geophysics, 39, 179–229, https://doi.org/https://doi.org/10.1029/1999RG000073, 2001.

Barnston, A. G. and Livezey, R. E.: Classification, Seasonality and Persistence of Low-Frequency Atmospheric Circulation Patterns, Monthly Weather Review, 115, 1083 – 1126, https://doi.org/10.1175/1520-0493(1987)115<1083:CSAPOL>2.0.CO;2, 1987.

Broomhead, D. and King, G. P.: Extracting qualitative dynamics from experimental data, Physica D: Nonlinear Phenomena, 20, 217–236, https://doi.org/https://doi.org/10.1016/0167-2789(86)90031-X, 1986.

Burgers, G. and Stephenson, D. B.: The ‘normality’ of ENSO, Geophys. Res. Lett., 26, 1027–1030, https://doi.org/https://doi.org/10.1029/1999GL900161, 1999.

Da Costa, E. and De Verdiere, A. C.: The 7.7-year North Atlantic Oscillation, Quart. J. Roy. Meteorol. Soc., 128, 797–817, https://doi.org/https://doi.org/10.1256/003590002321042036, 2002.

de Viron, O., Dickey, J. O., and Ghil, M.: Global modes of climate variability, Geophysical Research Letters, 40, 1832–1837, https://doi.org/https://doi.org/10.1002/grl.50386, 2013.

Deser, C., Alexander, M. A., Xie, S.-P., and Phillips, A. S.: Sea Surface Temperature Variability: Patterns and Mechanisms, Annual Review of Marine Science, 2, 115–143, https://doi.org/10.1146/annurev-marine-120408-151453, 2010.

Di Capua, G., Kretschmer, M., Donner, R. V., van den Hurk, B., Vellore, R., Krishnan, R., and Coumou, D.: Tropical and mid-latitude teleconnections interactingwith the Indian summer monsoon rainfall: a theory-guided causal effect network approach, Earth System Dynamics, 11, 17–34, https://doi.org/10.5194/esd-11-17-2020, 2020a.

Di Capua, G., Runge, J., Donner, R. V., van den Hurk, B., Turner, A. G., Vellore, R., Krishnan, R., and Coumou, D.: Dominant patterns of interaction between the tropics and mid-latitudes in boreal summer: causal relationships and the role of timescales, Weather and Climate Dynamics, 1, 519–539, https://doi.org/10.5194/wcd-1-519-2020, 2020b.

Di Lorenzo, E., Xu, T., Zhao, Y., Newman, M., Capotondi, A., Stevenson, S., Amaya, D., Anderson, B., Ding, R., Furtado, J., Joh, Y., Liguori, G., Lou, J., Miller, A., Navarra, G., Schneider, N., Vimont, D., Wu, S., and Zhang, H.: Modes and Mechanisms of Pacific Decadal-Scale Variability, Annual Review of Marine Science, 15, 249–275, https://doi.org/https://doi.org/10.1146/annurev-marine-040422-084555, 2023.

Dijkstra, H. A. and Ghil, M.: Low-frequency variability of the large-scale ocean circulation: A dynamical systems approach, Reviews of Geophysics, 43, https://doi.org/https://doi.org/10.1029/2002RG000122, 2005.

Ding, Q. and Wang, B.: Circumglobal Teleconnection in the Northern Hemisphere Summer, Journal of Climate, 18, 3483 – 3505, https://doi.org/10.1175/JCLI3473.1, 2005.

Ding, R., Li, J., Tseng, Y.-h., Sun, C., and Xie, F.: Joint impact of North and South Pacific extratropical atmospheric variability on the onset of ENSO events, Journal of Geophysical Research: Atmospheres, 122, 279–298, https://doi.org/https://doi.org/10.1002/2016JD025502, 2017.

Docquier, D., Vannitsem, S., Ragone, F., Wyser, K., and Liang, X. S.: Causal links between Arctic sea ice and its potential drivers based on the rate of information transfer, Geophysical Research Letters, 49, e2021GL095 892, https://doi.org/10.1029/2021GL095892, 2022.

Docquier, D., Vannitsem, S., and Bellucci, A.: The rate of information transfer as a measure of ocean-atmosphere interactions, Earth System Dynamics, 14, 577–591, https://doi.org/10.5194/esd-14-577-2023, 2023.

Docquier, D., Di Capua, G., Donner, R. V., Pires, C. A. L., Simon, A., and Vannitsem, S.: A comparison of two causal methods in the context of climate analyses, Nonlinear Processes in Geophysics, 31, 115–136, https://doi.org/10.5194/npg-31-115-2024, 2024a.

Docquier, D., Massonnet, F., Ragone, F., Sticker, A., Fichefet, T., and Vannitsem, S.: Drivers of summer Arctic sea-ice extent in CMIP6 large ensembles revealed by information flow, Scientific Reports, 14, https://doi.org/10.1038/s41598-024-76056-y, 2024b.

Efron, B. and Tibshirani, R.: An Introduction to the Bootstrap, Chapman and Hall, 1993.

Enfield, D. B., Mestas-Nuñez, A. M., Mayer, D. A., and Cid-Serrano, L.: How ubiquitous is the dipole relationship in tropical Atlantic sea surface temperatures?, Journal of Geophysical Research, 104, 7841–7848, https://doi.org/10.1029/1998JC900109, 1999.

Enfield, D. B., Mestas-Nuñez, A. M., and Trimble, P. J.: The Atlantic Multidecadal Oscillation and its relation to rainfall and river flows in the continental U.S., Geophysical Research Letters, 28, 2077–2080, https://doi.org/10.1029/2000GL012745, 2001.

Fraedrich, K., Pawson, S., and Wang, R.: An EOF Analysis of the Vertical-Time Delay Structure of the Quasi-Biennial Oscillation, Journal of Atmospheric Sciences, 50, 3357 – 3365, https://doi.org/10.1175/1520-0469(1993)050<3357:AEAOTV>2.0.CO;2, 1993.

García-Serrano, J., Cassou, C., Douville, H., Giannini, A., and Doblas-Reyes, F. J.: Revisiting the ENSO teleconnection to the Tropical North Atlantic, Journal of Climate, 30, 6945–6957, https://doi.org/10.1175/JCLI-D-16-0641.1, 2017.

Ghil, M., Allen, M. R., Dettinger, M. D., Ide, K., Kondrashov, D., Mann, M. E., Robertson, A. W., Saunders, A., Tian, Y., Varadi, F., and Yiou, P.: Advanced spectral methods for climatic time series, Reviews of Geophysics, 40, 41 pages, https://doi.org/10.1029/2000RG000092, 2002.

Graystone, P.: Meteorological office discussion on tropical meteorology, Meteorol. Mag, 88, 113–119, 1959.

Hagan, D. F. T., Wang, G., Liang, X. S., and Dolman, H. A. J.: A time-varying causality formalism based on the Liang–Kleeman information flow for analyzing directed interactions in nonstationary climate systems, J. Climate, 32, 7521–7537, https://doi.org/10.1175/JCLI-D-18-0881.1, 2019.

Hagan, D. F. T., Dolman, H. A. J., Wang, G., Lim Kam Sian, K. T. C., Yang, K., Ullag, W., and Shen, R.: Contrasting ecosystem constraints on seasonal terrestrial CO2 and mean surface air temperature causality projections by the end of the 21st century, Environmental Research Letters, 17, 124 019, https://doi.org/10.1088/1748-9326/aca551, 2022.

Hannachi, A., Straus, D. M., Franzke, C. L. E., Corti, S., and Woollings, T.: Low-frequency nonlinearity and regime behavior in the Northern Hemisphere extratropical atmosphere, Reviews of Geophysics, 55, 199–234, https://doi.org/https://doi.org/10.1002/2015RG000509, 2017.

Huang, Y., Franzke, C. L. E., Yuan, N., and Fu, Z.: Systematic identification of causal relations in high-dimensional chaotic systems: application to stratosphere-troposphere coupling, Climate Dynamics, 55, 2469–2481, https://doi.org/10.1007/s00382-020-05394-0, 2020a.

Huang, Y., Fu, Z., and Franzke, C. L. E.: Detecting causality from time series in a machine learning framework, Chaos: An Interdisciplinary Journal of Nonlinear Science, 30, 063 116, https://doi.org/10.1063/5.0007670, 2020b.

Jajcay, N., Kravtsov, S., Sugihara, G., Tsonis, A. A., and Paluš, M.: Synchronization and causality across time scales in El Niño Southern Oscillation, npj Climate and Atmospheric Science, 1, 33, 2018.

Johnson, Z. F., Chikamoto, Y., Wang, S.-Y. S., McPhaden, M. J., and Mochizuki, T.: Pacific decadal oscillation remotely forced by the equatorial Pacific and the Atlantic Oceans, Climate Dynamics, 55, 789–811, https://doi.org/10.1007/s00382-020-05295-2, 2020.

Kaplan, A., Cane, M., Kushnir, Y., Clement, A., Blumenthal, M., and Rajagopalan, B.: Analyses of global sea surface temperature 1856-1991, Journal of Geophysical Research, 103, 18 567–18 589, https://doi.org/10.1029/97JC01736, 1998.

Krakovská, A., Jakubík, J., Chvosteková, M., Coufal, D., Jajcay, N., and Paluš, M.: Comparison of six methods for the detection of causality in a bivariate time series, Physical Review E, 97, 042 207, https://doi.org/10.1103/PhysRevE.97.042207, 2018.

Kravtsov, S., Kondrashov, D., and Ghil, M.: Multilevel Regression Modeling of Nonlinear Processes: Derivation and Applications to Climatic Variability, Journal of Climate, 18, 4404 – 4424, https://doi.org/10.1175/JCLI3544.1, 2005.

Kretschmer, M., Coumou, D., Donges, J. F., and Runge, J.: Using causal effect networks to analyze different Arctic drivers of midlatitude winter circulation, Journal of Climate, 29, 4069–4081, https://doi.org/10.1175/JCLI-D-15-0654.1, 2016.

Levine, A. F. Z., McPhaden, M. J., and Frierson, D. M. W.: The impact of the AMO on multidecadal ENSO variability, Geophysical Research Letters, 44, 3877–3886, https://doi.org/https://doi.org/10.1002/2017GL072524, 2017.

Liang, X. S.: Unraveling the cause-effect relation between time series, Physical Review E, 90, 052 150, https://doi.org/10.1103/PhysRevE.90.052150, 2014a.

Liang, X. S.: Entropy evolution and uncertainty estimation with dynamical systems, Entropy, 16, 3605–3634, https://doi.org/10.3390/e16073605, 2014b.

Liang, X. S.: Information flow and causality as rigorous notions ab initio, Physical Review E, 94, 052 201, https://doi.org/10.1103/PhysRevE.94.052201, 2016.

Liang, X. S.: Normalized multivariate time series causality analysis and causal graph reconstruction, Entropy, 23, 679, https://doi.org/10.3390/e23060679, 2021.

Liang, X. S. and Kleeman, R.: Information transfer between dynamical system components, Physical Review Letters, 95, 244 101, https://doi.org/10.1103/PhysRevLett.95.244101, 2005.

Liang, X. S., Chen, D., and Zhang, R.: Quantitative Causality, Causality-Aided Discovery, and Causal Machine Learning, Ocean-Land-Atmosphere Research, 2, 0026, https://doi.org/10.34133/olar.0026, 2023.

Mantua, N. J., Hare, S. R., Zhang, Y., Wallace, J. M., and Francis, R. C.: A Pacific interdecadal climate oscillation with impacts on salmon production, Bulletin of the American Meteorological Society, 78, 1069–1080, https://doi.org/10.1175/1520-0477(1997)078<1069:APICOW>2.0.CO;2, 1997.

Martín-Rey, M., Rodríguez-Fonseca, B., Polo, I., and F., K.: On the Atlantic–Pacific Niños connection: a multidecadal modulated mode, Climate Dynnamics, 43, 3163–3178, https://doi.org/10.1007/s00382-014-2305-3, 2014.

Mosedale, T. J., Stephenson, D. B., Collins, M., and Mills, T. C.: Granger causality of coupled climate processes: Ocean feedback on the North Atlantic Oscillation, Journal of Climate, 19, 1182–1194, 2006.

Newman, M., Compo, G. P., and Alexander, M. A.: ENSO-forced variability of the Pacific decadal oscillation, Journal of Climate, 16, 3853–3857, 2003.

Nguyen-Huy, T., Deo, R. C., Mushtaq, S., An-Vo, D.-A., and Khan, S.: Modeling the joint influence of multiple synoptic-scale, climate mode indices on Australian wheat yield using a vine copula-based approach, European journal of agronomy, 98, 65–81, 2018.

Nigam, S., Sengupta, A., and Ruiz-Barradas, A.: Atlantic-Pacific Links in Observed Multidecadal SST Variability: Is the Atlantic Multidecadal Oscillation?s Phase Reversal Orchestrated by the Pacific Decadal Oscillation?, Journal of Climate, 33, 5479 – 5505, https://doi.org/10.1175/JCLI-D-19-0880.1, 2020.

Okumura, Y., Xie, S.-P., Numaguti, A., and Tanimoto, Y.: Tropical Atlantic air-sea interaction and its influence on the NAO, Geophysical Research Letters, 28, 1507–1510, https://doi.org/https://doi.org/10.1029/2000GL012565, 2001.

Omrani, N.-E., Keenlyside, N., Bader, J., and Manzini, E.: Stratosphere key for wintertime atmospheric response to warm Atlantic decadal conditions, Climate Dynamics, 42, 649–663, 2014.

Omrani, N.-E., Keenlyside, N., Matthes, K., Boljka, L., Zanchettin, D., Jungclaus, J. H., and Lubis, S. W.: Coupled stratosphere-troposphere-Atlantic multidecadal oscillation and its importance for near-future climate projection, NPJ Climate and Atmospheric Science, 5, 59, 2022.

Park, J.-H. and Li, T.: Interdecadal modulation of El Niño–tropical North Atlantic teleconnection by the Atlantic multi-decadal oscillation, Climate Dynamics, 52, 5345–5360, 2019.

Pires, C. and Hannachi, A.: Independent Subspace Analysis of the Sea Surface Temperature Variability: Non-Gaussian Sources and Sensitivity to Sampling and Dimensionality, Complexity, 2017, 1–23, https://doi.org/http://dx.doi.org/10.1155/2017/3076810, 2017.

Pires, C. and Hannachi, A.: Bispectral analysis of nonlinear interaction, predictability and stochastic modelling with application to ENSO, Tellus A, 73, 1–30, https://doi.org/https://doi.org/10.1080/16000870.2020.1866393, 2021.

Pires, C. and Perdigão, R.: Non-Gaussian interaction information: estimation, optimization and diagnostic application of triadic wave resonance, Nonlin. Processes Geophys., 22, 87–108, https://doi.org/https://doi.org/10.5194/npg-22-87-2015, 2015.

Pires, C., Docquier, D., and Vannitsem, S.: A general theory to estimate information transfer in nonlinear systems, Physica D: Nonlinear Phenomena, 458, 133 988, https://doi.org/10.1016/j.physd.2023.133988, 2024.

Runge, J.: Causal network reconstruction from time series: From theoretical assumptions to practical estimation, Chaos, 28, 075 310, https://doi.org/10.1063/1.5025050, 2018.

Runge, J., Bathiany, S., Bollt, E., Camps-Valls, G., Coumou, D., Deyle, E., Glymour, C., Kretschmer, M., Mahecha, M. D., Muñoz-Marí, J., van Nes, E. H., Peters, J., Quax, R., Reichstein, M., Scheffer, M., Schölkopf, B., Spirtes, P., Sugihara, G., Sun, J., Zhang, K., and Zscheischler, J.: Inferring causation from time series in Earth system sciences, Nature Communications, 10, 2553, https://doi.org/10.1038/s41467-019-10105-3, 2019.

Scaife, A. A., Knight, J. R., Vallis, G. K., and Folland, C. K.: A stratospheric influence on the winter NAO and North Atlantic surface climate, Geophysical Research Letters, 32, https://api.semanticscholar.org/CorpusID:17782070, 2005.

Silini, R., Tirabassi, G., Barreiro, M., Ferranti, L., and Masoller, C.: Assessing causal dependencies in climatic indices, Climate Dynamics, 61, 79–89, https://doi.org/10.1007/s00382-022-06562-0, 2022.

Smirnov, D. A.: Generative formalism of causality quantifiers for processes, Physical Review E, 105, 034 209, 2022.

Stips, A., Macias, D., Coughlan, C., Garcia-Gorriz, E., and Liang, X. S.: On the causal structure between CO_2 and global temperature, Scientific Reports, 6, https://doi.org/10.1038/srep21691, 2016.

Stuecker, M.: The climate variability trio: stochastic fluctuations, El Niño, and the seasonal cycle, Geosci. Lett., 10, 51, https://doi.org/10.1186/s40562-023-00305-7, 2023.

Thompson, D. W. J. and Wallace, J. M.: The Arctic oscillation signature in the wintertime geopotential height and temperature fields, Geophysical Research Letters, 25, 1297–1300, https://doi.org/https://doi.org/10.1029/98GL00950, 1998.

Timmermann, A. et al.: El Niño–Southern Oscillation complexity, Nature, 559, 535–545, https://doi.org/10.1038/s41586-018-0252-6, 2018.

Tsonis, A. A. and Swanson, K. L.: Review article "On the origins of decadal climate variability: a network perspective", Nonlinear Processes in Geophysics, 19, 559–568, https://doi.org/10.5194/npg-19-559-2012, 2012.

Tyrovolas, M., Liang, X. S., and Stylios, C.: Information flow-based fuzzy cognitive maps with enhanced interpretability, Granular Computing, 8, 2021–2038, 2023.

van Nes, E. H., Scheffer, M., Brovkin, V., Lenton, T. M., Ye, H., Deyle, E., and Sugihara, G.: Causal feedbacks in climate change, Nature Climate Change, 5, 445–448, https://doi.org/10.1038/NCLIMATE2568, 2015.

Vannitsem, S. and Ekelmans, P.: Causal dependences between the coupled ocean–atmosphere dynamics over the tropical Pacific, the North Pacific and the North Atlantic, Earth System Dynamics, 9, 1063–1083, https://doi.org/10.5194/esd-9-1063-2018, 2018.

Vannitsem, S. and Ghil, M.: Evidence of coupling in ocean-atmosphere dynamics over the North Atlantic, Geophysical Research Letters, 44, 2016–2026, https://doi.org/https://doi.org/10.1002/2016GL072229, 2017.

Vannitsem, S. and Liang, X. S.: Dynamical dependencies at monthly and interannual time scales in the climate system: Study of the North Pacific and Atlantic regions, Tellus A, 74, 141–158, https://doi.org/10.16993/tellusa.44, 2022.

Vannitsem, S., Dalaiden, Q., and Goosse, H.: Testing for dynamical dependence: Application to the surface mass balance over Antarctica, Geophysical Research Letters, 46, 12 125–12 135, https://doi.org/10.1029/2019GL084329, 2019.

Vannitsem, S., Pires, C. A., and Docquier, D.: Causal dependencies and Shannon entropy budget: Analysis of a reduced-order atmospheric model, Quarterly Journal of the Royal Meteorological Society, n/a, https://doi.org/https://doi.org/10.1002/qj.4805, 2024.

Vautard, R., Yiou, P., and Ghil, M.: Singular-spectrum analysis: A toolkit for short, noisy chaotic signals, Physica D: Nonlinear Phenomena, 58, 95–126, 1992.

Wallace, J. M. and Gutzler, D. S.: Teleconnections in the Geopotential Height Field during the Northern Hemisphere Winter, Monthly Weather Review, 109, 784 – 812, https://doi.org/10.1175/1520-0493(1981)109<0784:TITGHF>2.0.CO;2, 1981.

Wang, G., Swanson, K. L., and Tsonis, A. A.: The pacemaker of major climate shifts, Geophysical Research Letters, 36, L07 708, https://doi.org/https://doi.org/10.1029/2008GL036874, 2009.

Wang, J., Luo, H., Yu, L., Li, X., Holland, P. R., and Yang, Q.: The Impacts of Combined SAM and ENSO on Seasonal Antarctic Sea Ice Changes, Journal of Climate, 36, 3553 – 3569, https://doi.org/10.1175/JCLI-D-22-0679.1, 2023.

Wu, J., Ren, H.-L., Jia, X., and Zhang, P.: Climatological diagnostics and subseasonal-to-seasonal predictions of Madden–Julian Oscillation events, International Journal of Climatology, 43, 2449–2464, https://doi.org/https://doi.org/10.1002/joc.7984, 2023.

Wyatt, M., Kravtsov, S., and Tsonis, A. A.: Atlantic Multidecadal Oscillation and Northern Hemisphere's climate variability, Climate Dynamics, 38, 929–949, https://doi.org/10.1007/s00382-011-1071-8, 2012.

Zhao, S., Jin, F.-F., Stuecker, M. F., Thompson, P. R., Kug, J.-S., McPhaden, M. J., Cane, M. A., Wittenberg, A. T., and Cai, W.: Explainable El Niño predictability from climate mode interactions, Nature, 630, 891—898, https://doi.org/10.1038/s41586-024-07534-6, 2024.

Zscheischler, J., Westra, S., van den Hurk, B., Seneviratne, S. I., Ward, P. J., Pitman, A. J., Aghakouchak, A., Bresch, D. N., Leonard, M., Wahl, T., and Zhang, X.: Future climate risk from compound events, Nature Climate Change, 8, 469–477, https://api.semanticscholar.org/CorpusID:91131733, 2018.

Table 3. List of climate indices and their quadratic products that have a significant influence on the targets mentioned in the first row. These are listed by order of importance based on the mean value of the rate of information transfer (over 1000 bootstraps). These estimates are shown in Figs 3 and 6, as well as in the figures in the supplementary document. The value for the dominant influence is given between parentheses. In the first row, the results with the use of 44 predictors on the original series are displayed, while in the second row, the results with 44 predictors on the low-frequency variability series. Note that for the AMO, the influence of TNA in parenthesis with the set of nonlinear predictors is still intense but only at the 5% level.

Targets:	**NAO**	**AO**	**PNA**	**AMO**	**PDO**
Influences from	AO (0.027)	-	AO (0.012) Niño3.4	TNA (-0.27)	Niño3.4 (0.076) AO
Influences from	~~PNA*TNA~~PNA TNA(0.044) ~~TNA*QBO~~ TNA QBO ~~PNA*AMO~~ PNA AMO ~~AMO*QBO~~ AMO QBO PDO PNA QBO ~~AMO**2~~ AMO^2 ~~PNA*QBO~~ PNA QBO ~~AO*QBO~~ AO QBO	NAO (-0.1) ~~TNA*QBO~~ TNA QBO ~~NAO*Niño3~~NAO Niño3.4 Niño3.4~~**2~~ ^{2} Niño3.4 ~~*PNA~~ PNA QBO PNA	PDO (-0.12) Niño3.4 ~~NAO*AMO~~ NAO AMO ~~NAO*TNA~~ NAO TNA ~~AMO*TNA~~ AMO TNA NAO ~~AMO**2~~ AMO^2 ~~PDO**2~~ PDO^2 ~~AMO*QBO~~ AMO QBO ~~TNA*QBO~~ TNA QBO ~~PNA*TNA~~ PNA TNA AO	(TNA) (-0.093) Niño3.4 (0.053) ~~AMO**2~~ AMO^2 PNA ~~PNA*AMO~~ PNA AMO ~~NAO**2~~ NAO^2	Niño3.4 (0.13) NAO TNA ~~AO*AMO~~ AO AMO ~~AO*PDO~~ AO PDO AO ~~NAO*AMO~~ NAO AMO QBO